RESEARCH ARTICLE   **Open Access**

CrossMark

The distinctive cell division interactome of *Neisseria gonorrhoeae*

Yinan Zou[1,2], Yan Li[2,3] and Jo-Anne R. Dillon[1,2,3]*

Abstract

Background: Bacterial cell division is an essential process driven by the formation of a Z-ring structure, as a cytoskeletal scaffold at the mid-cell, followed by the recruitment of various proteins which form the divisome. The cell division interactome reflects the complement of different interactions between all divisome proteins. To date, only two cell division interactomes have been characterized, in *Escherichia coli* and in *Streptococcus pneumoniae*. The cell divison proteins encoded by *Neisseria gonorrhoeae* include FtsZ, FtsA, ZipA, FtsK, FtsQ, FtsI, FtsW, and FtsN. The purpose of the present study was to characterize the cell division interactome of *N. gonorrhoeae* using several different methods to identify protein-protein interactions. We also characterized the specific subdomains of FtsA implicated in interactions with FtsZ, FtsQ, FtsN and FtsW.

Results: Using a combination of bacterial two-hybrid (B2H), glutathione S-transferase (GST) pull-down assays, and surface plasmon resonance (SPR), nine interactions were observed among the eight gonococcal cell division proteins tested. ZipA did not interact with any other cell division proteins. Comparisons of the *N. gonorrhoeae* cell division interactome with the published interactomes from *E. coli* and *S. pneumoniae* indicated that FtsA-FtsZ and FtsZ-FtsK interactions were common to all three species. FtsA-FtsW and FtsK-FtsN interactions were only present in *N. gonorrhoeae*. The 2A and 2B subdomains of FtsA$_{Ng}$ were involved in interactions with FtsQ, FtsZ, and FtsN, and the 2A subdomain was involved in interaction with FtsW.

Conclusions: Results from this research indicate that *N. gonorrhoeae* has a distinctive cell division interactome as compared with other microorganisms.

Keywords: Cell division, Interactome, *N. gonorrhoeae*, Protein-protein interaction, Bacterial two-hybrid assay, Surface plasmon resonance, GST pull-down, FtsA domains

Background

Cell division is essential for bacterial survival. In *Escherichia coli* (Ec), normal cell division is driven by the formation of an FtsZ-ring at the division site [1], followed by the recruitment of other essential proteins, which together form the divisome [2]. Genes encoding most cell division proteins are located in a conserved region, the *d*ivision and *c*ell *w*all (*dcw*) cluster [3]. *dcw* clusters have been identified in most bacterial species, including *E. coli*, *Bacillus subtilis* (Bs), *Streptococcus pneumoniae* (Sp), *Caulobacter crescentus* (Cc) and *Neisseria gonorrhoeae*

(Ng) [4–7]. Although the gene organization of the *dcw* cluster varies in different bacteria species [8], proteins involved in the cell division process are relatively conserved [9, 10].

E. coli encodes ten essential cell division proteins, including FtsZ, FtsA, ZipA, FtsK, FtsQ, FtsB, FtsL, FtsW, FtsI, and FtsN [11, 12]. Assembly of the FtsZ-ring structure is initiated with the polymerization of FtsZ, driven by GTP hydrolysis, at the mid-cell [13]. FtsA and ZipA are recruited by FtsZ and anchor FtsZ to the inner membrane [14]. After the recruitment of FtsK, a DNA translocase involved in DNA segregation [15–17], the protein complexes FtsQ-FtsB-FtsL and FtsW-FtsI are localized to the septal ring, sequentially [15, 18]. Recent studies showed that the FtsQ-FtsB-FtsL complex serves as a signal sensor which promotes cell wall remodeling necessary for cell constriction [19]. FtsI is a high-molecular-

* Correspondence: j.dillon@usask.ca
[1]Department of Microbiology and Immunology, College of Medicine, Saskatoon, SK S7N 5E5, Canada
[2]Vaccine and Infectious Disease Organization, International Vaccine Centre, Saskatoon, SK S7N 5E3, Canada
Full list of author information is available at the end of the article

Zou *et al. BMC Microbiology* (2017) 17:232

Page 2 of 14

weight transpeptidase that cross-links glycan strands. The FtsW-FtsI complex is part of the peptidoglycan synthesis machinery, and FtsW, a lipid II flippase, transports the cell wall precursor across the membrane [20, 21]. FtsN is recruited as the last essential division protein that initiates cell constriction [22].

Using a bacterial two-hybrid (B2H) assay, an *E. coli* cell division protein-protein interaction network, the cell division interactome, which included 16 interactions between 10 cell divison proteins, was identified [23, 24]. The cell division interactome of *S. pneumoniae* was also characterized using a combination of B2H and co-immunoprecipitation assays [25]. A total of 17 interactions was observed among nine cell division proteins of *S. pneumoniae* which included FtsZ, FtsA, FtsK, DivIB, DivIC, FtsL, FtsW, and PBP2x [25]. To date, *E. coli* and *S. pneumoniae* are the only two organisms with characterized cell division interactomes [23–25].

N. gonorrhoeae is a Gram-negative diplococcus that causes gonorrhea in humans [26]. Previous studies on *N. gonorrhoeae* cell division focused on its Min system which localizes FtsZ to the mid-cell, and FtsZ [27–29]. *N. gonorrhoeae* also contains a *dcw* cluster which encodes 5 cell division proteins - FtsZ, FtsA, FtsQ, FtsW, and FtsI [7]. Other non-*dcw* cluster divisome proteins encoded by *N. gonorrhoeae* include ZipA, FtsK, and FtsN. As compared to *E. coli*, *N. gonorrhoeae* lacks FtsB and FtsL [7].

To investigate the cell division interactome in *N. gonorrhoeae*, its cell division protein interactions were identified using a combination of B2H and glutathione S-transferase (GST) pull-down assays, as well as surface plasmon resonance (SPR). We identified nine interactions among the eight cell division proteins tested. We also identified the subdomains of FtsA$_{Ng}$ involved in its interaction with FtsQ$_{Ng}$, FtsZ$_{Ng}$, FtsN$_{Ng}$, and FtsW$_{Ng}$. Comparison of the cell division interactomes of *E. coli*, *S. pneumoniae* and *N. gonorrhoeae* indicates that *N. gonorrhoeae* possesses a distinctive cell division interactome.

Methods
Strains and growth conditions
The bacterial strains and plasmids used in this study are shown in Table 1. *E. coli* DH5α and XL1-Blue were used as hosts for cloning. *E. coli* BL21 (DE3) and C41 (DE3) were used as hosts for protein purification. *E. coli* R721 was used in B2H assays [30]. *E. coli* DH5α, XL1-Blue, BL21(DE3) and C41 (DE3) were grown in Luria-Bertani (LB) medium (BD Difco™, Sparks, MD), for 16–18 h (hr), at 37 °C. *E. coli* R721 was grown under the same conditions and incubated at 34 °C, as described previously [24].

N. gonorrhoeae CH811 was grown on GC medium base agar (GCMB, Oakville, ON), supplemented with Kellogg's defined supplement (GCMBK, 40 g D-glucose,

1 g glutamine, 10 ml of 0.5% ferric nitrate and 1 ml of 20% cocarboxylase), at 35 °C, in a humid environment, with 5% CO_2, for 18 to 24 h [31].

When required, the following concentrations of antibiotics were added to LB medium: 100 μg/ml ampicillin (Sigma, Oakville, ON) or 50 μg/ml kanamycin (Sigma). For B2H assays, 34 μg/ml chloramphenicol (Sigma), 30 μg/ml kanamycin, and 50 μg/ml ampicillin were added to LB medium.

DNA manipulations
N. gonorrhoeae CH811 genomic DNA was purified using a QIAamp® genomic DNA kit (Qiagen, Mississauga, Ontario, Canada). DNA samples were stored at −20 °C. Oligonucleotides for polymerase chain reaction (PCR) amplifications were synthesized by Invitrogen (Table 2; Burlington, Ontario, Canada). PCRs were performed in a GeneAmp® PCR system 9700 (Applied Biosystems, Foster City, CA, USA) as follows: 4 min (min) at 94 °C, 30 cycles of denaturation for 1 min at 94 °C, annealing for 45 s (s) at 55 °C, extension for 1.5 mins at 72 °C, and 10 mins at 72 °C. PCRs were carried out in 100-μl (final volume) mixtures comprising 71.5 μl double-distilled H_2O (ddH_2O), 10 μl of 10× PCR buffer [15 mM $MgCl_2$, 4 μl of 10 mM deoxynucleoside triphosphate (dNTP), 2 μl of each primer (0.2 μg/ml), 0.5 μl of Taq DNA polymerase (5 U/μl; New England BioLabs, Ontario, Canada)], and, 10 μl of purified *N. gonorrhoeae* CH811 genomic DNA suspension.

Bacterial two-hybrid assays
The method developed by Di Lallo et al. [24] was used for all B2H assays. *ftsA*, *ftsK*, *ftsQ*, *ftsI*, *ftsW*, and *ftsN* were amplified from *N. gonorrhoeae* CH811 by PCR using the primer pairs P1/P2, P3/P4, P5/P6, P7/P8, P9/P10, and P11/P12 (Table 2), respectively. PCR amplicons were digested with BamHI and SalI and ligated into previously digested pcI$_{p22}$ and pcI$_{434}$ vectors, to produce pcl$_{p22}$-A, pcI$_{p22}$-K, pcI$_{p22}$-I, pcI$_{p22}$-W, pcI$_{p22}$-Q, pcI$_{p22}$-N, pcI$_{434}$-A, pcI$_{434}$-K, pcI$_{434}$-I, pcI$_{434}$-W, pcI$_{434}$-Q, and pcI$_{434}$-N (Table 3). *zipA*$_{Ng}$ was amplified from *N. gonorrhoeae* CH811 genomic DNA using the primer pair P13/P14 (Table 2); the PCR amplicons was digested with BglII and BamHI, and ligated into pre-digested pcI$_{p22}$ and pcI$_{434}$ to produce pcI$_{p22}$-ZipA and pcI$_{434}$-ZipA. pcI$_{p22}$-Z and pcI$_{434}$-Z constructs were generated previously [32].

The expression of *ftsA*$_{Ng}$, *ftsZ*$_{Ng}$ and *zipA*$_{Ng}$ from B2H constructs was verified by Western blot analysis using appropriate antibodies prepared in our lab using previously described methods [33]. These proteins were expressed from the vectors under the conditions tested (data not shown). The expression of these proteins indicated that any negative B2H interactions involving them was not a function of lack of expression.

Zou *et al. BMC Microbiology* (2017) 17:232

Page 3 of 14

Table 1 Bacterial strains used in this study

Stain	Relevant characteristics	Source/reference
E. coli DH5α	*supE44 ΔlacU169 (80lacZΔM15) hsdR17 endA1 gyrA96 thi-1 relA1*	Gibco
E. coli XL1-Blue	*recA1 endA1 gyrA96 thi-1 hsdR17 supE44 relA1 lac* [F' *proAB laclq ZΔM15*] Tn10	Stratagene
E. coli BL21(DE3)	F$^-$, *dcm* Δ, *ompT, hsdS* (r$_B^-$ m$_B^-$), *gal, λ(DE3)*	Stratagene
E. coli C41 (DE3)	F$^-$ *ompT hsdSB* (r$_B^-$ m$_B^-$) *gal dcm (srl-recA)* 306::Tn10 (Tet^r) *(DE3)*	[70]
E. coli R721	*supE thy D(lac-proAB)* F' [*proAB$^+$ lacl^q lac*ZDM15] *glpT*::O-$_{P434/P22}$*lacZ*	[30]
N. gonorrhoeae CH811	Auxotype (A)/serotype (S)/plasmid content (P) class: nonrequiring/IB-2/plasmid-free, Str^r	[71]

To ascertain what subdomains of FtsA$_{Ng}$ interacted with gonococcal cell division proteins FtsZ$_{Ng}$, FtsQ$_{Ng}$, FtsW$_{Ng}$, or FtsN$_{Ng}$, six previously created truncations of the protein (T1, T2, T3, T4, T5, and T6; Additional file 1: Figure S1) were used [33]. Plasmid constructs for B2H assays were previously generated [33].

B2H assays were performed as described previously [24]. This assay is based on the reconstitution of a chimeric repressor that binds to the 434/P22 hybrid operator and represses the expression of a downstream *lacZ* gene in *E. coli* R721. Each gene tested for a potential interaction was cloned into pcI$_{p22}$ and pcI$_{434}$ and recombinant constructs were transformed into *E. coli* R721 either singly or in combination. *N.*

gonorrhoeae FtsZ self-interaction was used as positive control. R721 without plasmids and single plasmid transformants were used as negative controls. R721 without plasmids had a β-galactosidase activity of 2504 ± 34 Miller units. The β-galactosidase activity of each combination was compared to that of R721. Values of less than 50% (<1250 Miller Units) indicate a positive interaction between two proteins, while values of more than 50% (>1250 Miller Units) indicate a negative interaction [24]. Statistical analyses were performed using the unpaired Student t-test. Standard deviations were determined for the mean value of Miller units where three independent experiments were performed.

Table 2 Primers designed in this study

Primer name		Sequences (5'-3')
P1	FtsA-reBamHI	GCGCGGATCCTCAGAGGTTGTTTTCAATCC
P2	FtsA-fwSalI	GCGCGTCGACCATGGAACAGCAGAAAAGATAC
P3	fwSalI-ftsK	GCGCGTCGACCATGTTTTGGATAGTTTTGATCGTTAT
P4	reBamHI-ftsK	CGCGGGATCCTCAAGCATTGTCCAAGGGGACGAG
P5	fwSalI-ftsQ	GCGCGTCGACCATGTGGGATAATGCCGAAGCGATG
P6	reBamHI-ftsQ	CGCGGGATCCCTATTCTTCGGATTCTTTTTCGGG
P7	fwSalI-ftsI	GCGCGTCGACCATGTTGATTAAAAGCGAATATAAGCC
P8	reBamHI-ftsI	CGCGGGATCCTTAAGACGGTGTTTTGACGGCTGC
P9	fwSalI-ftsW	GCGCGTCGACCATGAAGATTTCGGAAGTATTGGTAAA
P10	reBamHI-ftsW	CGCGGGATCCTTACTCCACCCGGTAACCGCGCAT
P11	fwSalI-ftsN	GCGCGTCGACCATGTTTATGAACAAATTTTCCCAATC
P12	reBamHI-ftsN	CGCGGGATCCTTATTTGCCTTCAATCGCACGGAT
P13	fwBglII-ZipA	GCGCGAGATCTGATGATTTACATCGTACTGTTCCTC
P14	reBamHI-ZipA	CGCGGGATCCTTATGAAAACAGGCGCAGGGC
P15	FtsA-reEcoRI-pET30a	ATATCGAATTCTCAGAGGTTGTTTTCAATCCACC
P16	FtsA-fwBglII-pET30a	AGCCCAGATCTGATGGAACAGCAGAAAAGATACATC
P17	fwBglII-FtsQ- pET30a	AGCCCAGATCTGATGTGGGATAATGCCGAAGCGATG
P18	reEcoRI-ftsQ- pET30a	ATATCGAATTCCTATTCTTCGGATTCTTTTTCGGG
P19	FtsZ-fwBgI II-pET30a	AGCCCAGATCTGATGGAATTTGTTTACGACGTGGCA
P20	FtsZ-ReEcoRI-pET30a	AGCCCGAATTCTTATTTGTCTGAATTGTGTTGACG
P21	fwFtsA-BamHI-GST	CGCGGGATCCATGGAACAGCAGAAAAGATACATC
P22	fwEcoRI-FtsN	GACGAATTCATGTTTATGAACAAATTTTCCCAATCC
P23	reXhoI-FtsN	GACCTCGAGTTATTTGCCTTCAATCGCACG

Zou *et al. BMC Microbiology* (2017) 17:232

Page 4 of 14

Table 3 Plasmids used in this study

Plasmid	Relevant genotype	Source/Reference
pcl$_{p22}$	pC132 derivative carrying N-terminal end of P22 repressor	[30]
pcl$_{434}$	pACYC177 derivative carrying N-terminal end of 434 repressor	[30]
pcl$_{p22}$-A	pclp22 derivative carrying the *ftsA$_{Ng}$* gene	This study
pcl$_{434}$-A	pcl$_{434}$ derivative carrying the *ftsA$_{Ng}$* gene	This study
pcl$_{p22}$-K	pclp22 derivative carrying the *ftsK$_{Ng}$* gene	This study
pcl$_{434}$-K	pcl$_{434}$ derivative carrying the *ftsK$_{Ng}$* gene	This study
pcl$_{p22}$-Q	pclp22 derivative carrying the *ftsQ$_{Ng}$* gene	This study
pcl$_{434}$-Q	pcl$_{434}$ derivative carrying the *ftsQ$_{Ng}$* gene	This study
pcl$_{p22}$-I	pclp22 derivative carrying the *ftsI$_{Ng}$* gene	This study
pcl$_{434}$-I	pcl$_{434}$ derivative carrying the *ftsI$_{Ng}$* gene	This study
pcl$_{p22}$-W	pclp22 derivative carrying the *ftsW$_{Ng}$* gene	This study
pcl$_{434}$-W	pcl$_{434}$ derivative carrying the *ftsW$_{Ng}$* gene	This study
pcl$_{p22}$-N	pclp22 derivative carrying the *ftsN$_{Ng}$* gene	This study
pcl$_{434}$-N	pcl$_{434}$ derivative carrying the *ftsN$_{Ng}$* gene	This study
pcl$_{p22}$-Z	pclp22 derivative carrying the *ftsZ$_{Ng}$* gene	[32]
pcl$_{434}$-Z	pcl$_{434}$ derivative carrying the *ftsZ$_{Ng}$* gene	[32]
pcl$_{p22}$-AT1	pclp22 derivative carrying the *ftsA$_{Ng}$* gene fragment encoding amino acids 1–162	[33]
pcl$_{p22}$-AT2	pclp22 derivative carrying the *ftsA$_{Ng}$* gene fragment encoding amino acids 1–194	[33]
pcl$_{p22}$-AT3	pclp22 derivative carrying the *ftsA$_{Ng}$* gene fragment encoding amino acids 1–230	[33]
pcl$_{p22}$-AT4	pclp22 derivative carrying the *ftsA$_{Ng}$* gene fragment encoding amino acids 231–301	[33]
pcl$_{p22}$-AT5	pclp22 derivative carrying the *ftsA$_{Ng}$* gene fragment encoding amino acids 302–414	[33]
pcl$_{p22}$-AT6	pclp22 derivative carrying the *ftsA$_{Ng}$* gene fragment encoding amino acids 351–414	[33]
pcl$_{434}$-AT1	pcl$_{434}$ derivative carrying the *ftsA$_{Ng}$* gene fragment encoding amino acids 1–162	[33]
pcl$_{434}$-AT2	pcl$_{434}$ derivative carrying the *ftsA$_{Ng}$* gene fragment encoding amino acids 1–194	[33]
pcl$_{434}$-AT3	pcl$_{434}$ derivative carrying the *ftsA$_{Ng}$* gene fragment encoding amino acids 1–230	[33]
pcl$_{434}$-AT4	pcl$_{434}$ derivative carrying the *ftsA$_{Ng}$* gene fragment encoding amino acids 231–301	[33]
pcl$_{434}$-AT5	pcl$_{434}$ derivative carrying the *ftsA$_{Ng}$* gene fragment encoding amino acids 302–414	[33]
pcl$_{434}$-AT6	pcl$_{434}$ derivative carrying the *ftsA$_{Ng}$* gene fragment encoding amino acids 351–414	[33]
pET30a	Kan^R P$_{T7}$::6Xhis	EMD Millipore, Billerica, MA
pETA	pET30a derivative carrying the *ftsA$_{Ng}$* gene	This study
pETQ	pET30a derivative carrying the *ftsQ$_{Ng}$* gene	This study
pETZ	pET30a derivative carrying the *ftsZ$_{Ng}$* gene	This study
pGEX2T	Amp^{R}P$_{tac}$::*gst*::*lacIq*	Amersham Bioscience, Uppsala, Sweden
pGEXA	pGEX2T derivative carrying the *ftsA$_{Ng}$* gene	This study
pGEXN	pGEX2T derivative carrying the *ftsA$_{Ng}$* gene	This study

Construction and purification of his-fusion proteins

For His-fusion constructs, full-length *ftsA, ftsQ,* and *ftsZ* were PCR-amplified from *N. gonorrhoeae* CH811 genomic DNA using primer pairs P15/P16, P17/P18 and P19/P20 (Table 2), respectively. PCR amplicons were digested with EcoRI and BglII and ligated into pre-digested pET30a, to create pETA, pETQ, and pETZ. Plasmid pETA was transformed into *E. coli* C41 (DE3) and plasmids pETQ and pETZ were transformed into *E. coli* BL21 (DE3). The overexpression of all fusion proteins was induced with 400 μM

IPTG, at 30 °C, for 2 h. Purification of His-FtsA$_{Ng}$, His-FtsZ$_{Ng}$, and His-FtsQ$_{Ng}$ was completed using His•Bind® Resin (EMD Millipore, Billerica, MA), following the manufacturer's instructions. His-FtsZ$_{Ng}$ was further treated with thrombin protease (EMD Millipore, Billerica, MA), overnight, at 4 °C, to cleave the N-terminal His tag. Thrombin was removed using 100 μl of p-aminobenzamidine-agarose (Sigma #A7155). FtsZ was dialyzed against MES buffer (50 mM MES, 300 mM KCl, 10 mM MgCl$_2$, pH 7.5) prior to use in FtsZ polymerization experiments [34].

Zou *et al. BMC Microbiology* (2017) 17:232

Page 5 of 14

GST pull-down assay

For GST fusion constructs, full-length *ftsA* and *ftsN* were PCR-amplified, from *N. gonorrhoeae* CH811, using primer pairs P21/P18 and P22/P23 (Table 2), respectively. The *ftsA* amplicon was digested with BamHI and EcoRI and ligated into pre-digested pGEX2T, to create pGEXA (Table 3). The *ftsN* amplicon was digested with EcoRI and XhoI and ligated into pre-digested pGEX2T, producing pGEXN (Table 3). Plasmids pGEXA and pGEXN were transformed into *E. coli* C41 (DE3) and *E. coli* BL21 (DE), respectively. Overexpression of GST-FtsA and GST-FtsN was accomplished by induction with either 400 μM or 800 μM of IPTG, respectively, at 30 °C, for 2 h. Purification of GST-FtsA and GST-FtsN was carried out using GST•Bind™ Resin (EMD Millipore, Billerica, MA), following the manufacturer's instructions.

Purified GST-fusion and His-fusion proteins were incubated with pre-equilibrated GST•Bind™ Resin in phosphate buffered saline (PBS) buffer (137 mM NaCl, 2.7 mM KCl, 10 mM Na_2HPO_4, 1.8 mM KH_2PO_4, 0.5% Triton-X100, 1 mM DTT, pH 7.9) at 4 °C overnight. Pre-purified GST was used as a negative control. The pre-bound resin was collected by centrifugation and washed in PBS three times. Bound proteins were dissociated from resin by adding 5X Laemmli buffer, separated by electrophoresis on 10% sodium dodecyl sulfate polyacrylamide gels (SDS-PAGE), and identified by Western blot using polyclonal anti-GST or anti-6 × His antibodies (Thermo Scientific; Waltham, MA), sequentially.

For $FtsA_{Ng}$-$FtsZ_{Ng}$ interactions, the GST pull-down assay was performed in MES buffer (50 mM MES-NaOH, 50 mM KCl, 10 mM $MgCl_2$, 0.5% Triton-X100, 1 mM ATP, 2 mM GTP, pH 7.5) [34]. To promote the polymerization of $FtsZ_{Ng}$ necessary for this interaction, $FtsZ_{Ng}$ was treated with 2 mM GTP and 1 mM ATP, as described previously [34], before mixing with GST-$FtsA_{Ng}$ and GST•Bind™ Resin.

All GST pull-down assays were performed minimally in duplicate.

FtsZ polymerization assays

$FtsZ_{Ng}$ polymerization was measured by 90° angle light scattering using a Dynapro-MS800 instrument (Wyatt Technology Corporation) with a wavelength of 310 nm and a slit width of 0.5 mm. MES buffer is optimal for FtsZ polymerization which is required to observe an FtsA-FtsZ interaction [34, 35]. $FtsZ_{Ng}$ (~6 μM) in MES buffer (50 mM MES-NaOH, 50 mM KCl, 10 mM $MgCl_2$, pH 7.5) was injected into a 45 ul quartz cuvette and warmed to 30 °C, prior to the measurement. Data were collected, for 4 min, from unpolymerized $FtsZ_{Ng}$ to establish a baseline. GTP was then added to a final concentration of 2 mM and data were collected every 5 s for 25 min. Data were recorded and analyzed using Dynamics v5 software.

Negative stain electron microscopy was used to visualize $FtsZ_{Ng}$ polymers. 5 μl of FtsZ (6 μM) with, or without, GTP (final concentration 2 mM) was incubated, at 30 °C, for 5 min. The mixture was placed on a carbon-coated copper grid (400 mesh size) for 2 min and then blot dried. The grid containing $FtsZ_{Ng}$ was stained with 1% uranyl acetate, blotted, and air-dried for 3 h. Polymers were visualized and photographed using a Hitachi transmission electron microscopy HT7700.

Surface plasmon resonance (SPR)

Protein interactions were examined by SPR using a Bio-Rad XPR36 (Bio-Rad Laboratories) instrument and a ProteOn™ HTE Sensor Chip (Bio-Rad Laboratories). The chip surface was regenerated by injection of 0.5% SDS, 50 mM NaOH, 100 mM HCl and 300 mM EDTA, at a flow rate of 30 μl/min, for 120 s. Activation was performed using 500 μM of $NiSO_4$.

For $FtsA_{Ng}$-$FtsN_{Ng}$ and $FtsA_{Ng}$-$FtsQ_{Ng}$ SPR experiments, ligands (i.e. His-$FtsN_{Ng}$ for $FtsA_{Ng}$-$FtsN_{Ng}$, and His-$FtsQ_{Ng}$ for $FtsA_{Ng}$-$FtsQ_{Ng}$ interactions) were immobilized onto the sensor chip at a concentration of 200 nM. A two-fold dilution series of the analyte ($FtsA_{Ng}$), in PBS buffer with Tween-20 (PBST; 137 mM NaCl, 2.7 mM KCl, 10 mM Na_2HPO_4, 1.8 mM KH_2PO_4, 0.1% BSA, 0.05% Tween-20, pH 7.9), was injected at a flow rate of 30 μl/min over the surface of the chip for 120 s. This was followed by an injection of PBST buffer for 300 s. Negative controls comprised a reference channel flowed with PBST buffer, and a chip surface immobilized with either $FtsQ_{Ng}$ or $FtsN_{Ng}$ flowed with GST in PBST.

For the $FtsA_{Ng}$-$FtsZ_{Ng}$ interaction, the SPR binding assay was performed using MES buffer, supplemented with 0.1% BSA, 0.05% Tween-20, and 1 mM ATP were added with the pH adjusted to 7.5. $FtsA_{Ng}$ was immobilized on the chip surface as described above. Each 120-s injection of polymerized $FtsZ_{Ng}$ was followed by an injection of supplemented MES buffer for 300 s for dissociation. Negative controls included a reference channel which was flowed with MES buffer containing 2 mM GTP, and the $FtsA_{Ng}$-immobilized chip surface flowed with GST in supplemented MES instead of polymerized $FtsZ_{Ng}$.

All SPR data was analyzed using ProteOn Manager™ (Bio-Rad Laboratories). The sensorgram (i.e. a graph of the response unit versus time) was first subtracted by the response units (RU) of the reference channel, with no immobilized ligands, to reduce the non-specific binding signals between analyte and empty chip surface. Then, the sensorgram was subtracted with the RU signal with running buffer and ligand immobilized on the chip. Association and disassociation constants were obtained using the Langmuir 1:1 kinetic fit model, by nonlinear regression, using ProteOn Manager™. Each protein pair was tested minimally in duplicate.

Zou *et al. BMC Microbiology* (2017) 17:232

Page 6 of 14

Results

Identification of *N. gonorrhoeae* cell division protein interactions by bacterial two-hybrid assay

Using B2H assays, we investigated 28 potential interactions among eight gonococcal divisome proteins including FtsZ, FtsA, ZipA, FtsK, FtsQ, FtsI, FtsW, and FtsN. The results (Table 4) show that nine interactions, FtsZ-FtsA, FtsZ-FtsK, FtsZ-FtsW, FtsA-FtsK, FtsA-FtsQ, FtsA-FtsW, FtsA-FtsN, FtsI-FtsW, and FtsK-FtsN, displayed a residual β-galactosidase activity lower than 50%, indicating a positive interaction between these proteins in *N. gonorrhoeae.* The interaction between $FtsA_{Ng}$ and $FtsN_{Ng}$ had the lowest residual β-galactosidase activity (24%), indicating the strongest interaction. This was followed by $FtsA_{Ng}$-$FtsK_{Ng}$ (30%), $FtsN_{Ng}$-$FtsK_{Ng}$ (31%), $FtsI_{Ng}$-$FtsW_{Ng}$ (35%), $FtsZ_{Ng}$-$FtsW_{Ng}$ (39%), $FtsA_{Ng}$-$FtsZ_{Ng}$ (40%), $FtsZ_{Ng}$-$FtsK_{Ng}$ (41%), $FtsA_{Ng}$-$FtsW_{Ng}$ (45%), and $FtsA_{Ng}$-$FtsQ_{Ng}$ (48%) interactions. $ZipA_{Ng}$ did not directly interact with other cell division proteins as the residual β-galactosidase activity of all interactions was above 50% (Table 4).

GST pull-down of $FtsA_{Ng}$-$FtsQ_{Ng}$, $FtsA_{Ng}$-$FtsZ_{Ng}$ and $FtsA_{Ng}$-$FtsN_{Ng}$ interactions

To confirm the results of selected B2H assays, we examined several interactions (i.e. $FtsQ_{Ng}$-$FtsA_{Ng}$, $FtsA_{Ng}$-$FtsN_{Ng}$, $FtsA_{Ng}$-$FtsZ_{Ng}$) using GST pull-down assays. GST pull-down results (Fig. 1a) showed that His-$FtsQ_{Ng}$ was pulled down by GST-$FtsA_{Ng}$, but not GST itself (negative control), indicating an interaction between $FtsA_{Ng}$ and $FtsQ_{Ng}$. Using similar evaluation criteria, we ascertained that His-$FtsA_{Ng}$ was pulled down

by GST-$FtsN_{Ng}$, indicating an interaction between these two proteins (Fig. 1b).

The interactions of $FtsA_{Ng}$ and $FtsZ_{Ng}$ from *E. coli* in vitro requires the presence of both ATP and GTP [35]. GTP promotes FtsZ polymerization, and ATP is necessary for FtsA to interact with FtsZ, but not for FtsZ polymerization [36, 37]. The presence of $FtsZ_{Ng}$ polymers in MES buffer was determined by transmission electron microscopy (TEM) and dynamic light scattering (DLS; Additional file 2: Figure S2). GST pull-down assay did not detect an interaction between $FtsA_{Ng}$ and $FtsZ_{Ng}$ in the presence of 1 mM ATP and 2 mM GTP (Fig. 1c). This result was unexpected, given our B2H results and the commonality of FtsA-FtsZ interaction in other bacterial species [24, 25, 38, 39], as ascertained by different in vivo assays (i.e. B2H, yeast two-hybrid, chemical cross-linking with co-immunoprecipitation).

Surface plasmon resonance evaluation of $FtsA_{Ng}$-$FtsQ_{Ng}$, $FtsA_{Ng}$-$FtsZ_{Ng}$ and $FtsA_{Ng}$-$FtsN_{Ng}$ interactions

Surface plasmon resonance (SPR) was used to confirm selected gonococcal cell division protein-protein interactions in real-time. SPR was used to evaluate the interactions of $FtsA_{Ng}$ with $FtsZ_{Ng}$ because of the conflicting results observed with B2H and GST pull-down assays. GTP was added to promote $FtsZ_{Ng}$ polymerization (Additional file 2: Figure S2). The sensorgram indicated that $FtsZ_{Ng}$ interacted with $FtsA_{Ng}$ at concentrations of 6 μM and 12 μM (Fig. 2a), but not at concentrations lower than 6 μM (data not shown). Kinetic analysis showed that the $FtsA_{Ng}$-$FtsZ_{Ng}$ interaction had a slow association ($ka = 3.56 \times 10^2$ M^{-1} s^{-1}) and a significant

Table 4 Interactions between eight cell division proteins in *N. gonorrhoeae* as determined by B2H assay

pcI_{P22}	pcI_{434}						
	ZipA	FtsZ	FtsA	FtsK	FtsI	FtsQ	FtsW
FtsZ	71±2.62%	28±0.27%					
FtsA	77±1.67%	40±2.46%[*]					
FtsK	78±2.45%	41±2.06%[*]	30±2.53%[*]				
FtsI	83±3.21%	91±3.92%	83±3.10%	76±2.00%			
FtsQ	100±4.04%	73±2.15%	48±2.59%[NS]	88±3.09%	90±2.82%		
FtsW	87±2.95%	39±2.66%[*]	45±3.29%[*]	100±2.62%	32±1.31%[*]	100±4.72%	
FtsN	100±2.78%	76±1.25%	24±1.66%[*]	31±0.67%[*]	100±4.82%	88±3.21%	97±2.10%

By comparison to positive controls (*E. coli* R721 without plasmids), interactions with less than 50% of residual ß-galactosidase activity (framed) were considered as positive. $FtsZ_{Ng}$ self-interaction was used as a positive control. The numbers represent percentage of mean ß-galactosidase activity, ± standard deviation
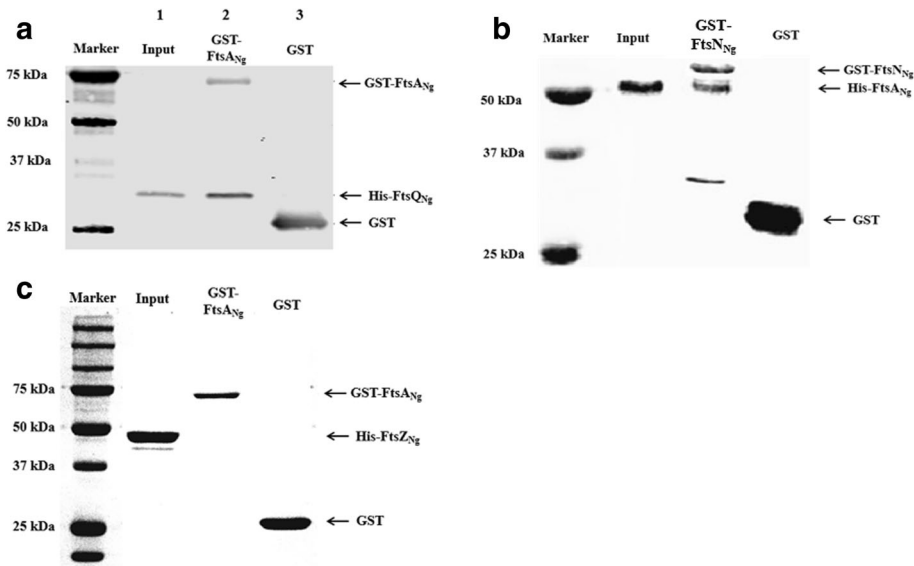[*]Statistically significant ($P \leq 0.05$); NS: not statistically significant ($P > 0.05$)

Fig. 1 Interactions of FtsA$_{Ng}$ with FtsQ$_{Ng}$, FtsN$_{Ng}$ and FtsZ$_{Ng}$ by GST pull-down. **a** GST pull down between His-FtsQ$_{Ng}$ and GST-FtsA$_{Ng}$. Lane 1: His-FtsQ$_{Ng}$ input; Lane 2: GST-FtsA$_{Ng}$ and His-FtsQ$_{Ng}$ mixture; Lane 3: GST and His-FtsQ$_{Ng}$ mixture; **b** GST pull down between His-FtsA$_{Ng}$ and GST-FtsN$_{Ng}$. Lane 1: His-FtsA$_{Ng}$ input; Lane 2: GST-FtsN$_{Ng}$ and His-FtsA$_{Ng}$ mixture, GST-FtsN$_{Ng}$ was loaded with GST and GST-FtsN$_{Ng}$ degradation products; Lane 3: GST and His-FtsA$_{Ng}$ mixture; **c** GST pull down between His-FtsZ$_{Ng}$ and GST-FtsA$_{Ng}$. Lane 1: His-FtsZ$_{Ng}$ input; Lane 2: GST-FtsA$_{Ng}$ and His-FtsZ$_{Ng}$ mixture; Lane 3: GST and His-FtsZ$_{Ng}$ mixture; His-tagged fusion proteins were visualized using anti-6 × His antibody; GST and GST-tagged fusion proteins were visualized using anti-GST antibody

disassociation activity (kd = 5.31×10^{-3} s^{-1}), giving a KD value of 14.9 μM. This suggested that the interaction between FtsA$_{Ng}$ and FtsZ$_{Ng}$ was likely transient. When GTP was absent from the FtsZ$_{Ng}$ protein solution, no binding was detected between FtsA$_{Ng}$ and FtsZ$_{Ng}$ (data not shown). The sensorgram of the interaction between FtsA$_{Ng}$ and the negative control (GST) also showed no binding activity (Fig. 2b), indicating the specificity of the SPR results for the interaction of FtsA$_{Ng}$ with FtsZ$_{Ng}$.
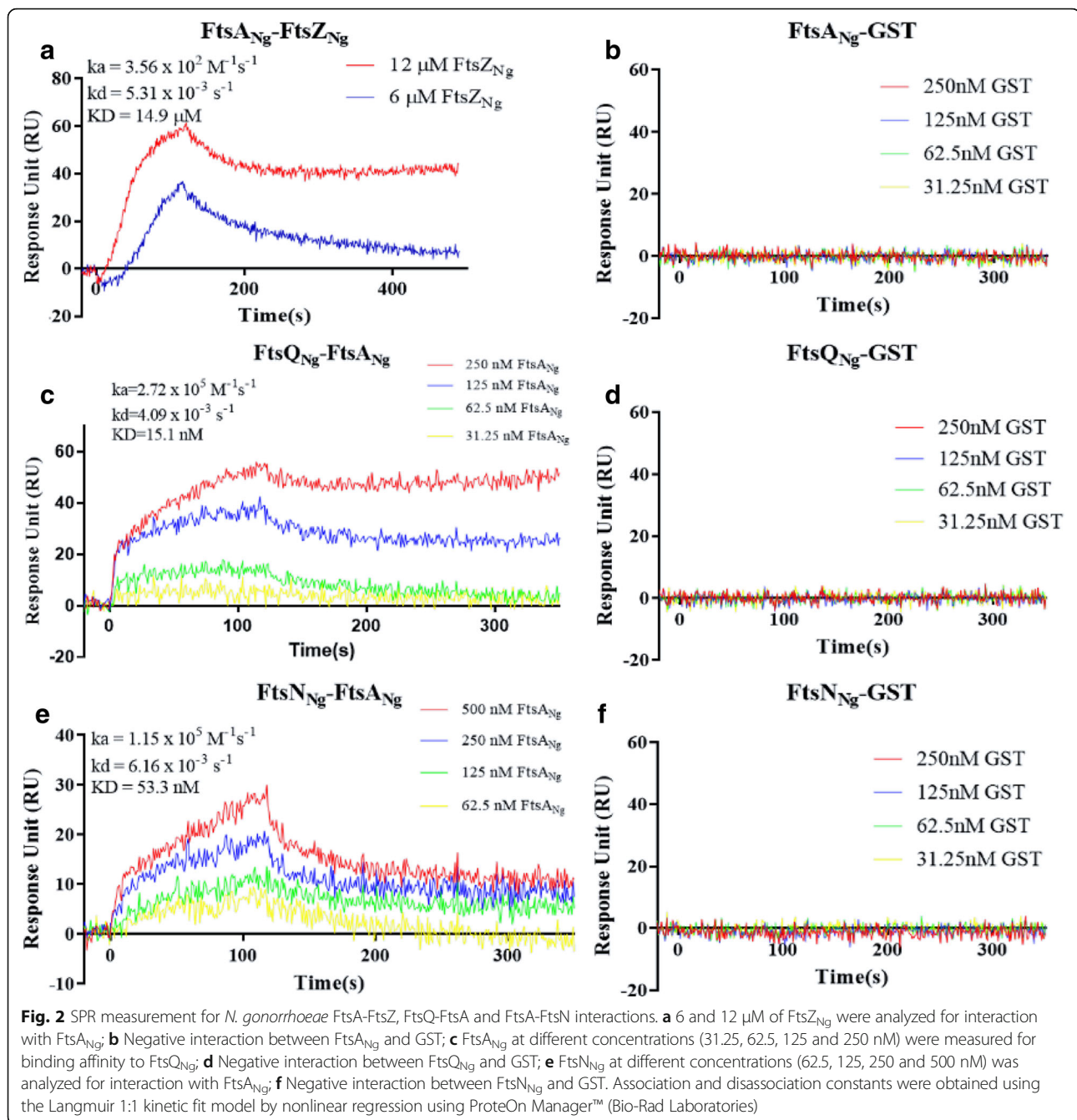
For the SPR analysis of the FtsA$_{Ng}$-FtsQ$_{Ng}$ interaction, FtsA$_{Ng}$ was tested using various concentrations (from 31.25 nM to 250 nM; Fig. 2c). At 0 s, the association of FtsA$_{Ng}$ and FtsQ$_{Ng}$ was observed immediately following injection of the FtsA$_{Ng}$ solution onto the FtsQ$_{Ng}$-labeled chip surface, with a rapid increase of response units (ka = 2.72×10^5 M^{-1} s^{-1}; Fig. 2c). This indicated a fast binding event between the two proteins. Disassociation between FtsA$_{Ng}$ and FtsQ$_{Ng}$ was not significant (kd = 4.09×10^{-3} s^{-1}), suggesting this interaction was strong and stable (KD = 15.1 nM). The negative control, using non-interacting GST, did not cause any change in the response units (Fig. 2d).

The FtsA$_{Ng}$-FtsN$_{Ng}$ interaction was observed with an increasing concentration of FtsA$_{Ng}$ (62.5 nM, 125 nM, 250 nM and 500 nM; Fig. 2e). His-FtsN$_{Ng}$ had a binding affinity (KD) of 53.3 nM with FtsA$_{Ng}$. The association and disassociation constants were 1.15×10^5 M^{-1} s^{-1}, and 6.16×10^{-3} s^{-1}, respectively (Fig. 2e), indicating a

strong interaction between FtsA$_{Ng}$ and FtsN$_{Ng}$. The injection of non-interacting GST onto the FtsN$_{Ng}$ immobilized chip surface did not cause any change in the response units (Fig. 2f).

The 2A and 2B subdomains of FtsA$_{Ng}$ interacts with FtsZ$_{Ng}$, FtsN$_{Ng}$, FtsW$_{Ng}$ and FtsQ$_{Ng}$

Since FtsA$_{Ng}$ interacted with FtsZ$_{Ng}$, FtsQ$_{Ng}$, FtsW$_{Ng}$, and FtsN$_{Ng}$, we further examined the interaction regions of FtsA$_{Ng}$ with these four proteins using B2H assays. Based on FtsA$_{Ng}$ homology modeling, six FtsA$_{Ng}$ truncations (T1-T6) were created (Additional file 1: Figure S1), which contained one or more FtsA$_{Ng}$ subdomains [33]. FtsZ$_{Ng}$ self-interaction was used as a positive control. And negative controls included *E. coli* R721 without plasmids or carrying each single recombinant B2H vector in which the gene of interest had been cloned. FtsA$_{Ng}$ truncations T3, T4, and T5 interacted with FtsZ$_{Ng}$ and FtsN$_{Ng}$ (Figs. 3 and 4, blue bars). FtsA$_{Ng}$ truncations T1, T2, and T6 did not show an interaction with these proteins (Figs. 3 and 4, green bars). The T4 and T5 truncations included the 2B and 2A$_2$ subdomains of FtsA$_{Ng}$, suggesting that these subdomains of FtsA$_{Ng}$ interacted with both FtsZ$_{Ng}$ and FtsN$_{Ng}$. The T3 construct contained also contained the 2A$_1$ subdomain of FtsA$_{Ng}$, as compared to truncations T1 and T2, indicating that this subdomain was also involved in interactions with FtsZ$_{Ng}$ and FtsN$_{Ng}$. FtsQ$_{Ng}$ interacted only

Zou *et al. BMC Microbiology* (2017) 17:232

Page 8 of 14

Fig. 2 SPR measurement for *N. gonorrhoeae* FtsA-FtsZ, FtsQ-FtsA and FtsA-FtsN interactions. **a** 6 and 12 μM of FtsZ$_{Ng}$ were analyzed for interaction with FtsA$_{Ng}$; **b** Negative interaction between FtsA$_{Ng}$ and GST; **c** FtsA$_{Ng}$ at different concentrations (31.25, 62.5, 125 and 250 nM) were measured for binding affinity to FtsQ$_{Ng}$; **d** Negative interaction between FtsQ$_{Ng}$ and GST; **e** FtsN$_{Ng}$ at different concentrations (62.5, 125, 250 and 500 nM) was analyzed for interaction with FtsA$_{Ng}$; **f** Negative interaction between FtsN$_{Ng}$ and GST. Association and disassociation constants were obtained using the Langmuir 1:1 kinetic fit model by nonlinear regression using ProteOn Manager™ (Bio-Rad Laboratories)

with the T4 and T5 truncations of FtsA$_{Ng}$ (Fig. 5, blue bars), indicating that the 2B and 2A$_2$ subdomains, but not the 2A$_1$ subdomain, were required for the FtsA$_{Ng}$-FtsQ$_{Ng}$ interaction. Only the T5 truncation of FtsA$_{Ng}$ interacted with FtsW$_{Ng}$, suggesting that 2A$_2$ subdomain was involved in the interaction with FtsW$_{Ng}$ (Additional file 3: Figure S3). In summary, these results showed that the 2A$_1$, 2A$_2$ and 2B subdomains of FtsA$_{Ng}$ are required for its interaction with FtsN$_{Ng}$ and FtsZ$_{Ng}$. The FtsA$_{Ng}$ 2A$_2$ and 2B subdomains are required for interaction with FtsQ$_{Ng}$, and

the 2A$_2$ subdomain is involved in the interaction with FtsW$_{Ng}$.

Discussion

The *N. gonorrhoeae* cell division interactome described in our study is the third cell division interaction network identified in bacteria, in addition to *E. coli* and *S. pneumoniae* (Fig. 6a) [23–25]. Compared to the other two interactomes (Fig. 6b and c), fewer interaction protein pairs are identified in *N. gonorrhoeae* (Fig. 6a). Only nine interactions are present among the eight divisome

Zou et al. BMC Microbiology (2017) 17:232

Page 9 of 14
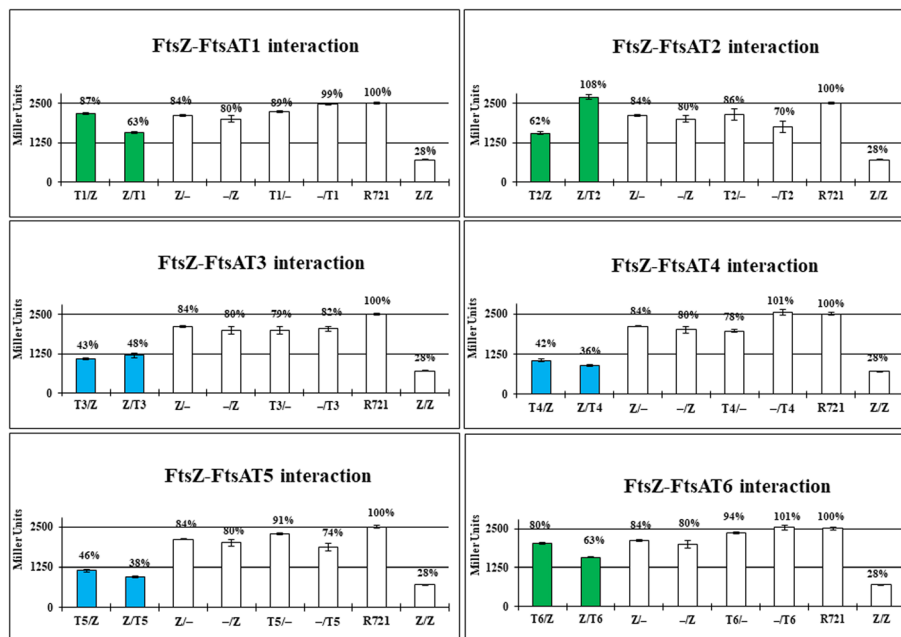
Fig. 3 Interactions between FtsA$_{Ng}$ truncations (T1, T2, T3, T4, T5 and T6) and FtsZ$_{Ng}$ (Z) by B2H assays. R721 without plasmids and single transformants were used as negative controls. R721 without plasmids had a β-galactosidase activity of 2504 ± 34 Miller units. FtsZ$_{Ng}$ self-interaction was used as a positive control. Values of less than 50% (<1250 Miller Unites) indicate a positive interaction between two proteins (blue bars) while values of more than 50% (>1250 Miller Unites) indicate a negative interaction (green bars) positive and negative controls are labeled in white (white bar)
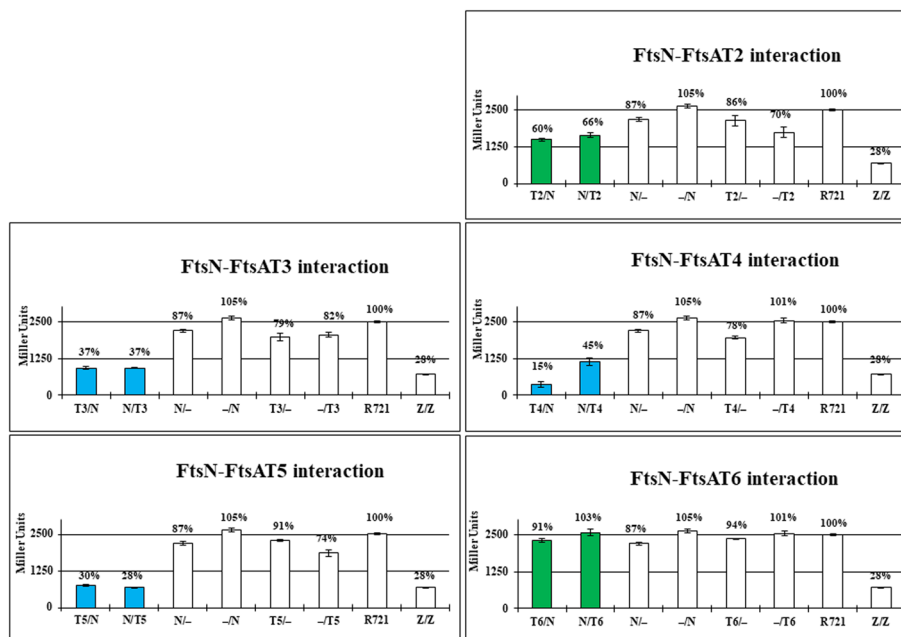
Fig. 4 Interactions between FtsA$_{Ng}$ truncations (T2, T3, T4, T5 and T6) and FtsN$_{Ng}$ (N) by B2H assays. Values of less than 50% (<1250 Miller Unites) indicate a positive interaction (blue bars) while values of more than 50% (>1250 Miller Unites) indicate a negative interaction (green bars)

Zou *et al. BMC Microbiology* (2017) 17:232

Page 10 of 14
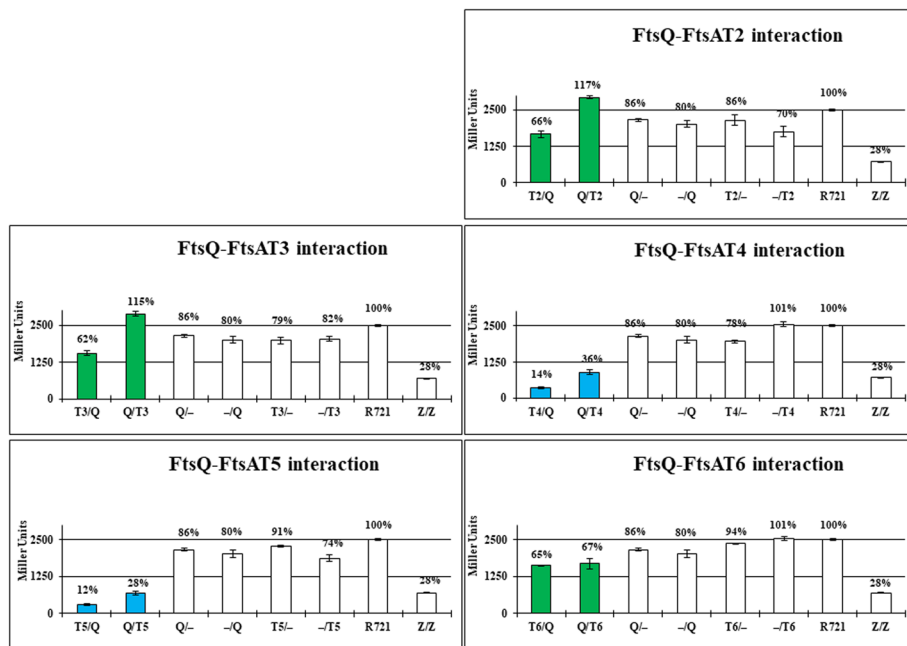
Fig. 5 Interactions between FtsA$_{Ng}$ truncations (T2, T3, T4, T5 and T6) and FtsQ$_{Ng}$ (Q) by B2H assays. Values of less than 50% (<1250 Miller Unites) indicate a positive interaction between two proteins (blue bars) while values of more than 50% (>1250 Miller Unites) indicate a negative interaction between the two proteins (green bars)
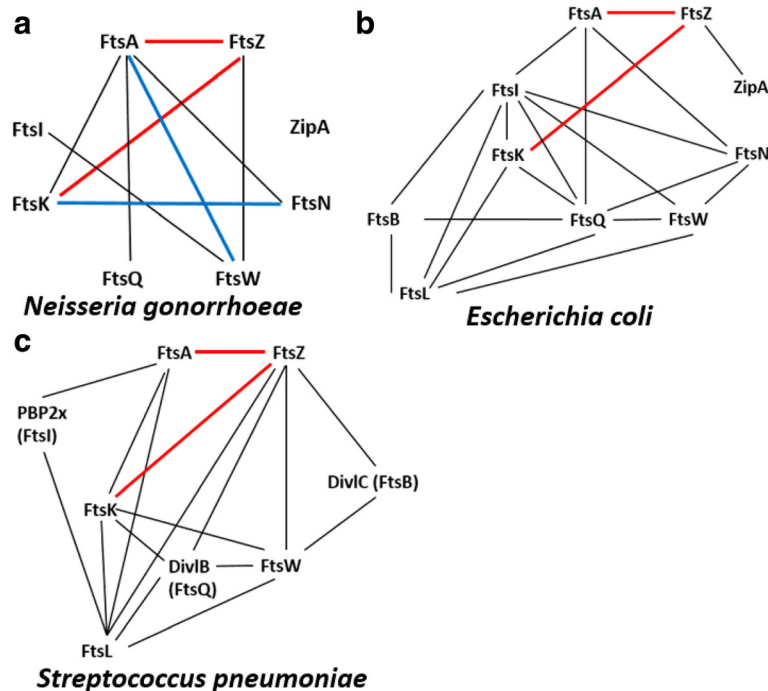
Fig. 6 Cell division interactomes of **a** *N. gonorrhoeae*, **b** *E. coli* [23, 24], and **c** *S. pneumoniae* [25]. Red lines indicate common interactions; blue lines indicate unique interactions in *N. gonorrhoeae*

Zou *et al. BMC Microbiology* (2017) 17:232

Page 11 of 14

proteins tested in *N. gonorrhoeae*, while *E. coli* and *S. pneumoniae* have 21 and 17 interactions among ten and eight divisome proteins, respectively [24, 25].

The development of all three cell division interactomes was based on interaction data obtained from the same B2H system [24, 25] The *E. coli* interactome was developed using B2H results exclusively while the *S. pneumoniae* study also applied co-immunoprecipitation to verify selected B2H positive interaction pairs [24, 25]. In our study, we used a combination of GST pull-down and surface plasmon resonance to further study selected positive B2H interactions.

Two interactions, FtsA-FtsZ and FtsZ-FtsK, are conserved in the cell division interactomes of *N. gonorrhoeae*, *E. coli* and *S. pneumoniae* (Fig. 6, red lines). The FtsA-FtsZ interaction is a common interaction in prokaryotes [24, 25, 39–41]. Both our B2H and SPR results confirmed this interaction in *N. gonorrhoeae*. A proper ratio between FtsA and FtsZ is crucial for the interaction in *E. coli* [42] and our SPR results support this finding; $FtsA_{Ng}$ interacts with $FtsZ_{Ng}$ only when its concentration is higher than 6 μM (Fig. 3b), indicating that the interaction requires a critical concentration threshold. Our SPR results further showed that interaction between $FtsA_{Ng}$ and $FtsZ_{Ng}$ was transient, a result warranting further study to fully understand its implications for divisome formation in *N. gonorrhoeae*. Unexpectedly, the GST pull-down assay, an in vitro assay, did not detect an $FtsA_{Ng}$-$FtsZ_{Ng}$ interaction. We believe that this "false negative" in vitro result was caused by the requirement of a membrane/solid surface support for the interaction to anchor FtsA [35, 43, 44].

The interaction of FtsZ with FtsK has been observed in *N. gonorrhoeae*, *E. coli*, *S. pneumoniae*, *B. subtilis* and *C. crescentus* [24, 25, 45, 46]. The C-terminus of FtsK is required for proper DNA segregation in *E. coli* [47]. The absence of an FtsZ-FtsK interaction in both *E. coli* and *C. crescentus* caused abnormal chromosome segregation and cell filamentation [45, 48]. This suggests that the FtsZ-FtsK interaction connects the cell division process with chromosome segregation, by ensuring that the replicated chromosome is cleared from the division site.

The FtsA-FtsW interaction has been observed only in *N. gonorrhoeae* (Fig. 6, blue lines). Since FtsW is a membrane protein and difficult to purify, we did not verify the interaction by GST pull-down and SPR assays. However, we performed additional B2H assays to identify which subdomains of FtsA were involved in its interaction with FtsW (Additional file 3: Figure S3) and showed that the $2A_2$ subdomain of FtsA strongly interacts with FtsW (Additional file 3: Figure S3). FtsW, an inner membrane protein, is required in *E. coli* for the recruitment of FtsI and the translocation of the cell well precursor, lipid II [20, 21, 49, 50]. An FtsI-FtsW protein

interaction has been observed in *E. coli*, *Streptomyces coelicolor*, and *Mycobacterium tuberculosis* [21, 51, 52]. Interestingly, we discovered that $FtsI_{Ng}$ only interacts with $FtsW_{Ng}$, suggesting that its localization may depend on this protein.

The importance of the unique $FtsK_{Ng}$-$FtsN_{Ng}$ interaction in *N. gonorrhoeae*, as determined by B2H, is not clear (Fig. 6, blue lines). In *E. coli*, FtsN is the last protein, of ten essential cell division proteins, recruited to the division site to initiate cell constriction [53, 54]. A previous study suggested that *E. coli* FtsN and FtsK stabilize the Z-ring cooperatively, without direct interactions [55]. Since the FtsK-FtsN interaction is present in *N. gonorrhoeae*, their joint involvement in gonococcal cell division requires further investigation.

$ZipA_{Ng}$ did not interact with any other gonococcal cell division protein. In *E. coli*, ZipA only interacts with FtsZ, and is required for downstream protein recruitment, including FtsK, FtsQ, FtsL, and FtsN [24, 56]. One report suggested that $ZipA_{Ng}$ is a homologue of the *E. coli* protein with high similarity in its key domains [57]. Although $ZipA_{Ng}$ complemented a conditional *zipA* mutant in *E. coli*, it did not fully restore a wild type phenotype in this strain [57]. Given these data, the role of ZipA in gonococcal cell division remains to be elucidated.

In *N. gonorrhoeae*, the existence of $FtsL_{Ng}$ is unclear due to its low homology with *E. coli* FtsL [58]. An open reading frame (ORF) located between *mraW* and *ftsI* in the *dcw* cluster of *N. gonorrhoeae* was reported by Francis et al. [7] and they reported that it was not a coding ORF. Snyder et al. [58] named the same ORF *ftsL*. Because this ORF shares only 17% amino acid similarity to its *E. coli* homologue, we considered that it was not a functional ORF and did not test its interaction with other gonococcal cell division proteins.

N. gonorrhoeae lacks FtsB [7]; thus, the protein complex FtsQ-B-L, present in other species, such as *E. coli*, *S. pneumoniae* and *B. subtilis*, would not be formed in *N. gonorrhoeae* [59–61]. This protein complex has been described as a bridge connecting FtsK and the FtsI-FtsW complex in *E. coli* [18]. A recent study suggests that the *E. coli* FtsQ-B-L complex acts as a signal transmitter for cell wall remodeling and constriction, which is mediated by direct interactions with the FtsI-W complex and FtsN [19]. In *S. pneumoniae*, the FtsQ homologue, DivIB, interacts with $FtsK_{Sp}$, $FtsL_{Sp}$, and $FtsW_{Sp}$ [25]. Interestingly, our B2H data show that $FtsQ_{Ng}$ only interacts with $FtsA_{Ng}$, suggesting that the function of $FtsQ_{Ng}$ in cell division in *N. gonorrhoeae* may be distinct.

There are several models for bacterial cell constriction. One *E. coli* model suggests that the force that drives constriction comes from septal peptidoglycan synthesis [62]. In this model, the $FtsA_{Ec}$-$FtsN_{Ec}$ interaction

Zou *et al. BMC Microbiology* (2017) 17:232

Page 12 of 14

activates peptidoglycan synthesis by direct or indirect interaction with $FtsI_{Ec}$ [63]. Another *E. coli* model suggests that the energy generated from FtsZ-mediated GTP hydrolysis drives cell constriction [43]. We observed an $FtsA_{Ng}$-$FtsN_{Ng}$ interaction in *N. gonorrhoeae*. However, there is no further evidence supporting either model of cell constriction in *N. gonorrhoeae* at this time.

The non-essential proteins, $FtsE_{Ng}$ and $FtsX_{Ng}$, are also implicated in cell division in *N. gonorrhoeae* [64]. Similarly, in *E. coli*, FtsE and FtsX are non-essential for cell division under conditions of high osmotic pressure [65]. Gonococcal FtsE and FtsX have high similarity in amino acid sequence to known homologues in other species [64]. In *E. coli*, the interaction between FtsE and FtsZ has a regulatory effect on the Z-ring [65]. Future research could focus on revealing the effects of $FtsE_{Ng}$ and $FtsX_{Ng}$ on cell division in *N. gonorrhoeae*.

The major issue interpreting B2H assay results is the empirical cut-off of 50% residual ß-galactosidase activity used to discriminate positive and negative interactions. In particular, values close to the cut-off could be interpreted as either false positive or negative results. To validate our B2H results, we used other B2H interactions to test which subdomains of $FtsA_{Ng}$ interacted with $FtsZ_{Ng}$, $FtsN_{Ng}$, and $FtsQ_{Ng}$. We determined that the 2A and 2B subdomains of $FtsA_{Ng}$ interacted with $FtsZ_{Ng}$, $FtsQ_{Ng}$, and $FtsN_{Ng}$. We also evaluated some positive interactions obtained by B2H using SPR and GST pull-down assays. The SPR method detects and measures weak or transient interactions, in real-time, with high sensitivity [66]. The SPR method showed a transient $FtsA_{Ng}$-$FtsZ_{Ng}$ interaction. GST pull-down assays, on the other hand, are ideal in detecting strong protein-protein interactions, as weak interactions may dissociate during the assay [67]. We consider this to be a reasonable explanation for our failure to confirm when the interaction of $FtsA_{Ng}$ with $FtsZ_{Ng}$ when using a GST pull-down assay.

To date, most of studies on cell division have been focused on model organisms (i.e. the Gram-negative rod *E. coli* and the Gram-positive rod *B. subtilis*) due to the abundant availability of tools for genetic manipulation [62]. Research on cell division in non-model organisms is expanding, and this includes studies with *N. gonorrhoeae* [7, 27]. For example, *Chlamydia trachomatis*, which lacks FtsZ, requires an actin-like protein, MreB, for cell division [68]. A gene cluster encoding three cell division proteins, named MldA, MldB, and MldC, was identified only in *Clostridium difficile* and its closely related bacteria [69]. Results from studies using non-model organisms suggest that cell division mechanisms are complex and vary in different organisms, reflecting vast biological diversity.

Conclusions

In our research, we discovered that nine interactions among eight cell division proteins defined the cell division interactome of *N. gonorrhoeae*. In comparison with the published cell division interactomes of *E. coli* and *S. pneumoniae*, FtsA-FtsZ and FtsZ-FtsK interactions were common to all three bacteria. FtsK-FtsN and FtsA-FtsW interactions were only present in *N. gonorrhoeae*, suggesting that they play different roles in the cell division of this microorganism. $ZipA_{Ng}$ did not interact with any other cell division proteins tested in this study, indicating that its role may differ as compared to its *E. coli* homologue. We also determined that the subdomains of $FtsA_{Ng}$ which interacted with $FtsQ_{Ng}$, $FtsZ_{Ng}$, $FtsW_{Ng}$, or $FtsN_{Ng}$, differed from its *E. coli* homologue. This suggests that *N. gonorrhoeae* possesses a distinctive cell division interactome, and likely a different mechanism of cell division as compared to *E. coli* and other organisms.

Additional files

Additional file 1: Figure S1. Schematic representation of *N. gonorrhoeae ftsA* and its truncations [33]. T1 (162aa, Met1-Ala162) contained the N-terminal 1A and 1C domains of $ftsA_{Ng}$. T2 (194aa, Met1-Val194) included the N-terminal 1A, 1C and 1A domains of $ftsA_{Ng}$. T3 (230aa, Met1-Ile230) included the N-terminal 1A, 1C, 1A and $2A_1$ domains of $ftsA_{Ng}$. T4 (71aa, Pro231-Glu301) contained the 2B domain of $ftsA_{Ng}$. T5 (114aa, Ile301-Leu414) contained the $2A_2$ and 1A C-terminal domains of $ftsA_{Ng}$. T6 (64aa, Ala351-Leu414) contained the 1A C-terminal domain of $ftsA_{Ng}$. (DOCX 30 kb)

Additional file 2: Figure S2. $FtsZ_{Ng}$ polymerization assays. $FtsZ_{Ng}$ polymers visualized by transmission electron microscope with(A) or without (B) 2 mM GTP in MES buffer (50 mM MES-NaOH, 50 mM KCl, 10 mM $MgCl_2$, pH 7.5) at 30 °C. Solid arrows indicate $FtsZ_{Ng}$ polymers. Scale bar indicates 100 nm. (C) Light scattering of $FtsZ_{Ng}$ polymerization (6 µM) in MES buffer. (DOCX 211 kb)

Additional file 3: Figure S3. Interactions between $FtsA_{Ng}$ truncations (T2, T3, T4, T5 and T6) and $FtsW_{Ng}$ (W) by B2H assay. Values of less than 50% (<1250 Miller Units) indicate a positive interaction between two proteins (blue bars) while values of more than 50% (>1250 Miller Units) indicate a negative interaction (green bars). (DOCX 66 kb)

Zou *et al. BMC Microbiology* (2017) 17:232

Page 13 of 14

Availability of data and materials
The data from this report are included within the article. Datasets used in the current study are available upon request.

Authors' contributions
YZ and YL participated in the experimental design, implementation and data analysis. YZ also wrote the first draft of manuscript. JRD designed and supervised the entire project and was responsible for the final submission of the manuscript. All authors contributed to manuscript revisions. All authors have read and approved the final manuscript.

Ethics approval and consent to participate
Ethics approval is not required for this study. Consent to participate is not applicable.

Consent for publication
Not applicable.

Competing interests
The authors declare that they have no competing interests.

Publisher's Note
Springer Nature remains neutral with regard to jurisdictional claims in published maps and institutional affiliations.

Author details
[1]Department of Microbiology and Immunology, College of Medicine, Saskatoon, SK S7N 5E5, Canada. [2]Vaccine and Infectious Disease Organization, International Vaccine Centre, Saskatoon, SK S7N 5E3, Canada. [3]Department of Biology, College of Arts and Science, University of Saskatchewan, Saskatoon, SK S7N 5A5, Canada.

References
1. Lutkenhaus J, Addinall SG. Bacterial cell division and the Z ring. Annu Rev Biochem. 1997;66:93–116.
2. Margolin W. Themes and variations in prokaryotic cell division. FEMS Microbiol Rev. 2000;24:531–48.
3. Ayala J, Garrido T, de pedro MA, Vicente M. Molecular biology of bacterial septation. In: Ghuysen JM, Hakenbeck R, editors. New comprehensive Biochemistry; 1994. p. 73–101.
4. Mingorance J, Tamames J, Vicente M. Genomic channeling in bacterial cell division. J Mol Recognit. 2004;17:481–7.
5. Real G, Henriques AO. Localization of the *Bacillus subtilis* murB gene within the dcw cluster is important for growth and sporulation. J Bacteriol. 2006;188:1721–32.
6. Massidda O, Anderluzzi D, Friedli L, Feger G. Unconventional organization of the division and cell wall gene cluster of *Streptococcus pneumoniae*. Microbiology. 1998;144:3069–78.
7. Francis F, Ramirez-Arcos S, Salimnia H, Victor C, Dillon JA. Organization and transcription of the division cell wall (dcw) cluster in *Neisseria gonorrhoeae*. Gene. 2000;251:141–51.
8. Tamames J, González-Moreno M, Mingorance J, Valencia A, Vicente M. Bringing gene order into bacterial shape. Trends Genet. 2001;17:124–6.
9. Lutkenhaus J, Pichoff S, Du S. Bacterial cytokinesis: from Z ring to divisome. Cytoskeleton (Hoboken). 2012;69:778–90.
10. Haeusser DP, Margolin W. Splitsville: structural and functional insights into the dynamic bacterial Z ring. Nat Rev Microbiol. 2016;14:305–19.
11. Errington J, Daniel RA, Scheffers DJ. Cytokinesis in bacteria. Microbiol Mol Biol Rev. 2003;67:52–65.
12. Grenga L, Rizzo A, Paolozzi L, Ghelardini P. Essential and non-essential interactions in interactome networks: the *Escherichia coli* division proteins FtsQ-FtsN interaction. Environ Microbiol. 2013;15:3210–7.
13. Mukherjee M, Lutkenhaus J. Dynamic assembly of FtsZ regulated by GTP hydrolysis. EMBO J. 1998;17:462–9.
14. Hale CA, de Boer PA. Direct binding of FtsZ to ZipA, an essential component of the septal ring structure that mediates cell division in *E. coli*. Cell. 1997;88:175–85.
15. Goehring NW, Gonzalez MD, Beckwith J. Premature targeting of cell division proteins to midcell reveals hierarchies of protein interactions involved in divisome assembly. Mol Microbiol. 2006;61:33–45.
16. Begg KJ, Dewar SJ, Donachie WD. A new Escherichia coli cell division gene, ftsK. J Bacteriol. 1995;177:6211–22.
17. XC Y, Weihe EK, Margolin W. Role of the C terminus of FtsK in *Escherichia coli* chromosome segregation. J Bacteriol. 1998;180:6424–8.
18. Buddelmeijer N, Beckwith J. A complex of the Escherichia coli cell division proteins FtsL, FtsB and FtsQ forms independently of its localization to the septal region. Mol Microbiol. 2004;52:1315–27.
19. Tsang MJ, Bernhardt TG. A role for the FtsQLB complex in cytokinetic ring activation revealed by an ftsL allele that accelerates division. Mol Microbiol. 2015;95:925–44.
20. Mohammadi T, van Dam V, Sijbrandi R, Vernet T, Zapun A, Bouhss A, et al. Identification of FtsW as a transporter of lipid-linked cell wall precursors across the membrane. EMBO J. 2011;30:1425–32.
21. Fraipont C, Alexeeva S, Wolf B, van der Ploeg R, Schloesser M, den Blaauwen T, et al. The integral membrane FtsW protein and peptidoglycan synthase PBP3 form a subcomplex in *Escherichia coli*. Microbiology. 2011;157:251–9.
22. Vicente M, Rico AI. The order of the ring: assembly of *Escherichia coli* cell division components. Mol Microbiol. 2006;61:5–8.
23. Karimova G, Dautin N, Ladant D. Interaction network among *Escherichia coli* membrane proteins involved in cell division as revealed by bacterial two-hybrid analysis. J Bacteriol. 2005;187:2233–43.
24. Di Lallo G, Fagioli M, Barionovi D, Ghelardini P, Paolozzi L. Use of a two-hybrid assay to study the assembly of a complex multicomponent protein machinery bacterial septosome differentiation. Microbiology. 2003;149:3353–9.
25. Maggi S, Massidda O, Luzi G, Fadda D, Paolozzi L, Ghelardini P. Division protein interaction web: identification of a phylogenetically conserved common interactome between *Streptococcus pneumoniae* and *Escherichia coli*. Microbiology. 2008;154:3042–52.
26. Tapsall JW, Ndowa F, Lewis DA, Unemo M. Meeting the public health challenge of multidrug and extensively drug-resistant *Neisseria gonorrhoeae* that causes gonorrhea in humans. Expert Rev Anti-Infect Ther. 2009;7:821–34.
27. Salimnia H, Radia A, Bernatchez S, Beveridge TJ, Dillon JA. Characterization of the *ftsZ* cell division gene of *Neisseria gonorrhoeae*: expression in *Escherichia* Coli and *N. gonorrhoeae*. Arch Microbiol. 2000;173:10–20.
28. Ramirez-Arcos S, Szeto J, Beveridge TJ, Victor C, Francis F, Dillon JA. Deletion of the cell-division inhibitor MinC results in lysis of *Neisseria gonorrhoeae*. Microbiology. 2001;147:225–37.
29. Szeto J, Ramirez-Arcos S, Raymond C, Hicks LD, Kay CM, Dillon JA. Gonococcal MinD affects cell division in *Neisseria gonorrhoeae* and *Escherichia coli* and exhibits a novel self-interaction. J Bacteriol. 2001;183:6253–64.
30. Di Lallo G, Castagnoli L, Ghelardini P, Paolozzi L. A two-hybrid system based on chimeric operator recognition for studying protein homoheterodimerization in Escherichia coli. Microbiol. 2001;147:1651–6.
31. Kellogg DS, Peacock WL, Deacon WE, Brown L, Pirkle DI. *Neisseria gonorrhoeae*. I. Virulence genetically linked to clonal variation. J Bacteriol. 1963;85:1274–9.
32. Greco-Stewart V, Ramirez-Arcos S, Liao M, Dillon JR. N terminus determinants of MinC from Neisseria gonorrhoeae mediate interaction with FtsZ but do not affect interaction with MinD or homodimerization. Arch Microbiol. 2007;187:451–8.
33. Zou Y, Li Y, Ekanayake SB, Dillon JR. An Escherichia coli expression model reveals the species-specific function of FtsA from Neisseria gonorrhoeae in cell division. FEMS Microbiol Lett. 2017;364:fnx078.
34. Krol E, Scheffers DJ. FtsZ polymerization assays: simple protocols and considerations. J Vis Exp. 2013;81:e50844.
35. Loose M, Mitchison TJ. The bacterial cell division proteins FtsA and FtsZ self-organize into dynamic cytoskeletal patterns. Nat Cell Biol. 2014;16:38–46.
36. Pichoff S, Lutkenhaus J. Tethering the Z ring to the membrane through a conserved membrane targeting sequence in FtsA. Mol Microbiol. 2005;55:1722–34.
37. Beuria TK, Mullapudi S, Mileykovskaya E, Sadasivam M, Dowhan W, Margolin W. Adenine nucleotide-dependent regulation of assembly of bacterial tubulin-like FtsZ by a hypermorph of bacterial actin-like FtsA. J Biol Chem. 2009;284:14079–86.
38. Jensen SO, Thompson LS, Harry EJ. Cell division in *Bacillus subtilis*: FtsZ and FtsA association is Z-ring independent, and FtsA is required for efficient midcell Z-ring assembly. J Bacteriol. 2005;187:6536–44.

Zou *et al. BMC Microbiology* (2017) 17:232

Page 14 of 14

39. Yan K, Pearce KH, Payne DJ. A conserved residue at the extreme C-terminus of FtsZ is critical for the FtsA-FtsZ interaction in Staphylococcus aureus. Biochem Biophys Res Commun. 2000;270:387–92.

40. Gamba P, Veening JW, Saunders NJ, Hamoen LW, Daniel RA. Two-step assembly dynamics of the *Bacillus subtilis* divisome. J Bacteriol. 2009;191:4186–94.

41. Din N, Quardokus EM, Sackett MJ, Brun YV. Dominant C-terminal deletions of FtsZ that affect its ability to localize in Caulobacter and its interaction with FtsA. Mol Microbiol. 1998;27:1051–63.

42. Rueda S, Vicente M, Mingorance J. Concentration and assembly of the division ring proteins FtsZ, FtsA, and ZipA during the *Escherichia coli* cell cycle. J Bacteriol. 2003;185:3344–51.

43. Osawa M, Anderson DE, Erickson HP. Curved FtsZ protofilaments generate bending forces on liposome membranes. EMBO J. 2009;28:3476–84.

44. Arumugam S, Chwastek G, Fischer-Friedrich E, Ehrig C, Mönch I, Schwille P. Surface topology engineering of membranes for the mechanical investigation of the tubulin homologue FtsZ. Angew Chem Int Ed Eng. 2012;51:11858–62.

45. Wang SC, West L, Shapiro L. The bifunctional FtsK protein mediates chromosome partitioning and cell division in *Caulobacter*. J Bacteriol. 2006;188:1497–508.

46. Biller SJ, Burkholder WF. The *Bacillus subtilis* SftA (YtpS) and SpoIIIE DNA translocases play distinct roles in growing cells to ensure faithful chromosome partitioning. Mol Microbiol. 2009;74:790–809.

47. Sherratt DJ, Arciszewska LK, Crozat E, Graham JE, Grainge I. The *Escherichia coli* DNA translocase FtsK. Biochem Soc Trans. 2010;38:395–8.

48. Grenga L, Luzi G, Paolozzi L, Ghelardini P. The *Escherichia coli* FtsK functional domains involved in its interaction with its divisome protein partners. FEMS Microbiol Lett. 2008;287:163–7.

49. Mercer KL, Weiss DS. The *Escherichia coli* cell division protein FtsW is required to recruit its cognate transpeptidase, FtsI (PBP3), to the division site. J Bacteriol. 2002;184:904–12.

50. Mohammadi T, Sijbrandi R, Lutters M, Verheul J, Martin NI, den Blaauwen T, et al. Specificity of the transport of lipid II by FtsW in *Escherichia coli*. J Biol Chem. 2014;289:14707–18.

51. Mistry BV, Del Sol R, Wright C, Findlay K, Dyson P. FtsW is a dispensable cell division protein required for Z-ring stabilization during sporulation septation in *Streptomyces coelicolor*. J Bacteriol. 2008;190:5555–66.

52. Datta P, Dasgupta A, Singh AK, Mukherjee P, Kundu M, Basu J. Interaction between FtsW and penicillin-binding protein 3 (PBP3) directs PBP3 to mid-cell, controls cell septation and mediates the formation of a trimeric complex involving FtsZ, FtsW and PBP3 in mycobacteria. Mol Microbiol. 2006;62:1655–73.

53. Gerding MA, Liu B, Bendezu FO, Hale CA, Bernhardt TG, de Boer PA. Self-enhanced accumulation of FtsN at division sites and roles for other proteins with a SPOR domain (DamX, DedD, and RlpA) in *Escherichia coli* cell constriction. J Bacteriol. 2009;191:7383–401.

54. Rico AI, Garcia-Ovalle M, Palacios P, Casanova M, Vicente M. Role of *Escherichia coli* FtsN protein in the assembly and stability of the cell division ring. Mol Microbiol. 2010;76:760–71.

55. Goehring NW, Robichon C, Beckwith J. Role for the nonessential N terminus of FtsN in divisome assembly. J Bacteriol. 2007;189:646–9.

56. Hale CA, de Boer PAJ. ZipA is required for recruitment of FtsK, FtsQ, FtsL, and FtsN to the septal ring in Escherichia coli. J Bacteriol. 2002;184:2552–6.

57. Du Y, Arvidson CG. Identification of ZipA, a signal recognition particle-dependent protein from *Neisseria gonorrhoeae*. J Bacteriol. 2003;185:2122–30.

58. Snyder LA, Saunders NJ, Shafer WM. A putatively phase variable gene (dca) required for natural competence in Neisseria gonorrhoeae but not Neisseria meningitidis is located within the division cell wall (dcw) gene cluster. J Bacteriol. 2001;183:1233–41.

59. Daniel RA, Noirot-Gros MF, Noirot P, Errington J. Multiple interactions between the transmembrane division proteins of *Bacillus subtilis* and the role of FtsL instability in divisome assembly. J Bacteriol. 2006;188:7396–404.

60. Noirclerc-Savoye M, Le Gouellec A, Morlot C, Dideberg O, Vernet T, Zapun A. In Vitro reconstitution of a trimeric complex of DivIB, DivIC and FtsL, and their transient co-localization at the division site in *Streptococcus pneumoniae*. Mol Microbiol. 2005;55:413–24.

61. Robichon C, King GF, Goehring NW, Beckwith J. Artificial septal targeting of *Bacillus subtilis* cell division proteins in *Escherichia coli*: an interspecies approach to the study of protein-protein interactions in multiprotein complexes. J Bacteriol. 2008;190:6048–59.

62. Eswara PJ, Ramamurthi KS. Bacterial cell division: nonmodels poised to take the spotlight. Annu Rev Microbiol. 2017;71:393–411.

63. Liu B, Persons L, Lee L, de Boer PA. Roles for both FtsA and the FtsBLQ subcomplex in FtsN-stimulated cell constriction in *Escherichia coli*. Mol Microbiol. 2015;95:945–70.

64. Bernatchez S, Francis F, Salimnia H, Beveridge TJ, Li H, Dillon JA. Genomic, transcriptional and phenotypic analysis of ftsE and ftsX of *Neisseria gonorrhoeae*. DNA Res. 2000;7:75–81.

65. Corbin BD, Wang Y, Beuria TK, Margolin W. Interaction between cell division proteins FtsE and FtsZ. J Bacteriol. 2007;189:3026–35.

66. Ngounou Wetie AG, Sokolowska I, Woods AG, Roy U, Loo JA, Darie CC. Investigation of stable and transient protein-protein interactions: past, present, and future. Proteomics. 2013;13:538–57.

67. Bruckner A, Polge C, Lentze N, Auerbach D, Schlattner U. Yeast two-hybrid, a powerful tool for systems biology. Int J Mol Sci. 2009;10:2763–88.

68. Liechti G, Kuru E, Packiam M, Hsu YP, Tekkam S, Hall E, et al. Pathogenic chlamydia lack a classical sacculus but synthesize a narrow, mid-cell peptidoglycan ring, regulated by MreB, for cell division. PLoS Pathog. 2016;12:e1005590.

69. Ransom EM, Williams SB, Weiss DS, Ellermeier CD. Identification and characterization of a gene cluster required for proper rod shape, cell division, and pathogenesis in *Clostridium difficile*. J Bacteriol. 2014;196:2290–300.

70. Miroux B, Walker JE. Over-production of proteins in *Escherichia coli*: mutant hosts that allow synthesis of some membrane proteins and globular proteins at high levels. J Mol Biol. 1996;260:289–98.

71. Picard FJ, Dillon JA. Biochemical and genetic studies with arginine and proline auxotypes of *Neisseria gonorrhoeae*. Can J Microbiol. 1989;35:1069–75.